

## RESEARCH ARTICLES

# Regulation of Compound Leaf Development in *Medicago truncatula* by *Fused Compound Leaf1*, a Class M KNOX Gene

Jianling Peng,<sup>a</sup> Jianbin Yu,<sup>b,c,1</sup> Hongliang Wang,<sup>a,2</sup> Yingqing Guo,<sup>a</sup> Guangming Li,<sup>a</sup> Guihua Bai,<sup>b,c</sup> and Rujin Chen<sup>a,3</sup>

<sup>a</sup> Plant Biology Division, The Samuel Roberts Noble Foundation, Ardmore, Oklahoma 73401

<sup>b</sup> U.S. Department of Agriculture/Agricultural Research Service, Hard Winter Wheat Genetics Research Unit, Manhattan, Kansas 66506

<sup>c</sup> Department of Agronomy, Kansas State University, Manhattan, Kansas 66506

*Medicago truncatula* is a legume species belonging to the inverted repeat lacking clade (IRLC) with trifoliolate compound leaves. However, the regulatory mechanisms underlying development of trifoliolate leaves in legumes remain largely unknown. Here, we report isolation and characterization of *fused compound leaf1* (*fcl1*) mutants of *M. truncatula*. Phenotypic analysis suggests that *FCL1* plays a positive role in boundary separation and proximal-distal axis development of compound leaves. Map-based cloning indicates that *FCL1* encodes a class M KNOX protein that harbors the MEINOX domain but lacks the homeodomain. Yeast two-hybrid assays show that *FCL1* interacts with a subset of *Arabidopsis thaliana* BEL1-like proteins with slightly different substrate specificities from the *Arabidopsis* homolog KNATM-B. Double mutant analyses with *M. truncatula* *single leaflet1* (*sgl1*) and *palmate-like pentafoliata1* (*palm1*) leaf mutants show that *fcl1* is epistatic to *palm1* and *sgl1* is epistatic to *fcl1* in terms of leaf complexity and that *SGL1* and *FCL1* act additively and are required for petiole development. Previous studies have shown that the canonical KNOX proteins are not involved in compound leaf development in IRLC legumes. The identification of *FCL1* supports the role of a truncated KNOX protein in compound leaf development in *M. truncatula*.

## INTRODUCTION

Leaves are lateral organs initiated from the flanks of the shoot apical meristem (SAM). Leaf development can be divided into three successive and overlapping stages: initiation, in which leaves emerge from the flanks of the SAM; primary morphogenesis, in which the basic leaf form is determined; and secondary morphogenesis or histogenesis, in which leaves differentiate and produce cell types typical of mature leaves (Hagemann and Gleissberg, 1996; Poethig, 1997; Kaplan, 2001; Efroni et al., 2008; Efroni et al., 2010; Shani et al., 2010). Unlike the SAM's self-renewing nature, the growth of a leaf is determinate and lasts only for a limited duration.

Leaves exhibit a tremendous diversity in shape, size, and arrangement and can be classified as being either simple or compound, according to their complexities. A simple leaf has

a single continuous blade, and a compound leaf consists of multiple discontinuous blades, each resembling a simple leaf and known as a leaflet. The margin of a leaf or leaflet can be lobed, serrate, or entire (smooth), further elaborating the complexity of the leaf form.

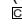
The class I *KNOTTED1-like* (*KNOXI*) homeobox transcription factor genes are required for the establishment and maintenance of the meristematic activity of the SAM (Long et al., 1996). For both simple- and compound-leaved species, leaf initiation requires downregulation of *KNOXI* genes at incipient leaf primordia (Long et al., 1996; Bharathan et al., 2002). This downregulation is permanent in simple-leaved species such as *Arabidopsis thaliana* and maize (*Zea mays*) (Lincoln et al., 1994). In most compound-leaved eudicot species, such as tomato (*Solanum lycopersicum*) and *Cardamine hirsuta* (an *Arabidopsis* relative with compound leaves), *KNOXI* gene expression is reactivated in developing leaf primordia (Bharathan et al., 2002; Hay and Tsiantis, 2006). Overexpression of *KNOXI* genes in the tomato-dominant mutants *Mouse Ears* and *Curl* (Chen et al., 1997; Parnis et al., 1997) or ectopic expression of *KNOXI* genes in tomato plants (Hareven et al., 1996; Janssen et al., 1998) results in a dramatic increase in leaf complexity. In *C. hirsuta*, downregulation of the *KNOXI* gene *SHOOT MERISTEMLESS* (*STM*) results in simplified leaves, whereas ectopic expression of *STM* results in more complex leaves (Hay and Tsiantis, 2006). These observations indicate that *KNOXI* genes are required for compound leaf development in these compound-leaved species.

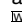
<sup>1</sup> Current address: Pioneer Hi-Bred International, Willmar, MN 56201.

<sup>2</sup> Current address: School of Life Sciences, Arizona State University, Tempe, AZ 85287.

<sup>3</sup> Address correspondence to rchen@noble.org.

The author responsible for distribution of materials integral to the findings presented in this article in accordance with the policy described in the Instructions for Authors (www.plantcell.org) is: Rujin Chen (rchen@noble.org).

 Some figures in this article are displayed in color online but in black and white in the print edition.

 Online version contains Web-only data.

www.plantcell.org/cgi/doi/10.1105/tpc.111.089128

The reactivation of *KNOX1* genes in leaf primordia in a large number of eudicot species that have compound leaves indicates a requirement for a transient phase of indeterminacy during compound leaf development (Bharathan et al., 2002; Champagne et al., 2007). However, the transient indeterminacy is not sufficient for compound leaf development, since it can also lead to simple leaves as a result of secondary morphogenesis in some species (Bharathan et al., 2002). Depending on the developmental context, ectopic expression of *TKNs*, the tomato *KNOX1* genes, has different effects on leaf shape, supporting a role for *TKNs* in stage-specific suppression of leaf maturation in tomato (Shani et al., 2009). In a large subclade of legumes, the inverted repeat-lacking clade (IRLC), which diverged from the basal Fabaceae ~39 million years ago and includes pea (*Pisum sativum*) and *Medicago truncatula*, *KNOX1* proteins are not detected in compound leaf primordia, suggesting that *KNOX1* genes are not likely associated with compound leaf development in this group of legumes (Hofer et al., 2001; Champagne et al., 2007).

Although conflicting evidence exists suggesting the expression of *KNOX1* genes in compound leaf primordia in *M. truncatula* (Di Giacomo et al., 2008), *UNIFOLIATA (UNI)* in pea and *SINGLE LEAFLET1 (SGL1)* in *M. truncatula*, both orthologous to the floral meristem identity genes *FLORICAULA (FLO)* and *LEAFY (LFY)*, have been shown to be required for compound leaf development in these legume species (Hofer et al., 1997; Wang et al., 2008). In *Lotus japonicus*, a legume outside of the IRLC clade, *proliferating floral meristem* mutants of the *FLO/LFY* ortholog also exhibit moderately reduced compound leaf phenotypes (Dong et al., 2005). In soybean (*Glycine max*), downregulation of the two *LFY* orthologs through RNA interference leads to a moderate reduction in leaflet number (Champagne et al., 2007). In tomato *fa* mutants, mutations in the tomato *LFY* ortholog lead to a reduced number of only secondary leaflets (Molinero-Rosales et al., 1999). These results support a role for *FLO/LFY* orthologs in compound leaf development in species-specific contexts. Interestingly, although *KNOX1* proteins are not detected in leaf primordia, the developmental program leading to compound leaves in alfalfa (*M. sativa*), an IRLC legume, is still responsive to ectopic expression of the tomato *KNOX1* gene *Le T6* (Champagne et al., 2007).

Increasing evidence supports that leaf development is responsive to genetic, hormonal, and environmental regulation (Efroni et al., 2010). Recently, it has been shown that local auxin accumulation is required for and precedes the initiation of leaf and leaflet primordia in diverse species (Barkoulas et al., 2008; Koenig et al., 2009). Interruption of auxin accumulation by auxin transport inhibitors or mutations in auxin carrier genes results in compromised initiation and development of leaf/leaflet primordia (DeMason and Chawla, 2004; Wang et al., 2005; Barkoulas et al., 2008; Koenig et al., 2009; Peng and Chen, 2011; Zhou et al., 2011). By contrast, external application of auxin promotes leaflet initiation and blade outgrowth (Koenig et al., 2009). The hormone cytokinin plays an important role in regulating the morphogenetic activity of compound leaves in tomato (Shani et al., 2010). Cytokinin acting downstream from *KNOX1* can substitute for *KNOX1* activity at leaf margins and regulates leaf shape in tomato. *NAM/CUC* genes encoding the NAC domain proteins play a conserved role in leaflet separation and leaf serration in diverse species (Blein et al., 2008; Berger et al., 2009). Down-

regulation of *NAM/CUC* genes by virus-induced gene silencing leads to different degrees of leaflet fusion, reduction of leaflet number, and smoothing of leaf margins (Blein et al., 2008). In tomato, loss-of-function mutations in *GOBLET*, the tomato ortholog of *CUC2*, lead to cotyledon and leaflet fusions (Blein et al., 2008; Berger et al., 2009). The role of *NAM/CUC* genes in leaf shape regulation is dependent on its regulation of *KNOX1* and *UNI* gene expression (Blein et al., 2008). In the IRLC legume, *M. truncatula PALMATE-LIKE PENTAFOLIATA1 (PALM1)* has been shown to encode a novel Cys(2)His(2) zinc finger transcription factor and plays a key role in regulating the morphogenetic activity of compound leaves through negative regulation of *SGL1* expression (Chen et al., 2010; Ge et al., 2010).

The canonical *KNOX1* protein contains conserved *KNOX1* and *KNOX2* domains, collectively called the MEINOX domain at its N terminus and the homeodomain at its C terminus. In *Arabidopsis* and tomato, class M *KNOX* proteins that lack the homeodomain have been identified recently (Kimura et al., 2008; Magnani and Hake, 2008). Ectopic expression of the *Arabidopsis* class M *KNOX* gene, *KNATM-B*, results in elongated petioles and narrow lamina (Magnani and Hake, 2008). By contrast, a gain-of-function mutation in the tomato class M *KNOX* gene, *PTS/TKD1*, results in a proliferation of compound leaves (Kimura et al., 2008). It has been shown that the class M *KNOX* genes function to interfere with the canonical *KNOX1* activity by titrating protein-protein interactions involving *KNOX1* and its interacting partners, BEL1-like (BELL) proteins, and by regulating nuclear localization of *KNOX1*-BELL complexes. However, the role of class M *KNOX1* in leaf development remains to be elucidated, since neither loss-of-function mutants nor knockdown mutants have been isolated in *Arabidopsis* and tomato (Kimura et al., 2008; Magnani and Hake, 2008). Here, we report the isolation and characterization of loss-of-function *fused compound leaf1 (fcl1)* mutants from *M. truncatula*. Our results indicate that the *M. truncatula FCL1* gene encodes a class M *KNOX* protein that has sequence similarity with the *Arabidopsis* *KNATM-B* and tomato *PTS/TKD1*. Our results further indicate that *FCL1* plays a key role in boundary separation and proximal-distal axis development of compound leaves in the legume. We show that both *FCL1* and *SGL1* are required for the development of petioles.

## RESULTS

### Isolation and Characterization of *M. truncatula fcl1* Mutants

To identify additional regulators of compound leaf development in legumes, we screened and isolated two similar leaf mutants, M368 and M602, from a deletion mutant collection in the model legume *M. truncatula* (cv Jemalong A17) derived from fast neutron bombardment mutagenesis (Wang et al., 2006). The majority of mature leaves developed in these two mutants were simplified with lobes due to leaflet fusion in contrast with the trifoliolate wild-type leaves (Figures 1A and 1B). A small number of mature leaves in *fcl1* mutants were single or had two leaflets fused or three leaflets clustered together without the rachis (Figure 1B). Based on subsequent genetic studies, we named M368 and M602, two recessive mutants, *fcl1-1* and *fcl1-2*, respectively.

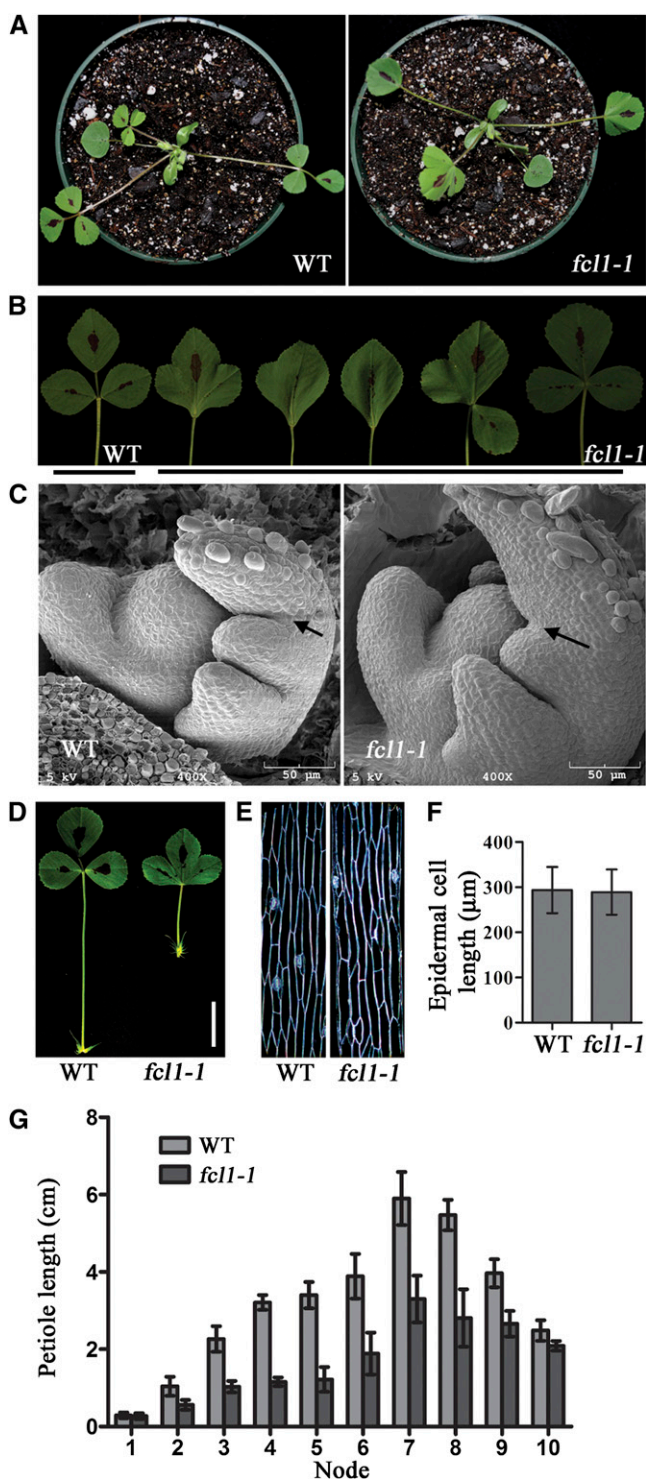


**Figure 1.** Phenotypic Characterization of *M. truncatula fcl1* Mutants.

**(A)** Three-week-old wild-type (WT) (Jemalong A17; left) and *fcl1-1* mutant (right).

**(B)** Close-up views of mature leaves of 2-month-old wild type and *fcl1-1* mutant, showing phenotypic variations within a single mutant plant compared with the trifoliolate wild-type leaf.

**(C)** Scanning electron microscopy images of wild-type (left) and

*fcl1-1* (right) compound leaf primordia. Arrows indicate the boundary between terminal and lateral leaflet primordia developed at the P2 stage.

To examine the early events in compound leaf development that are altered in *fcl1* mutants, we performed scanning electron microscopy analysis. The initiation of common leaf primordia from flanks of the SAM and the initiation of stipule and lateral leaflet primordia from the leaf margin appeared to be normal in the *fcl1* mutants compared with wild-type plants (Figure 1C). During a late P2 stage (P for Plastochron) when lateral leaflet primordia separated from the terminal leaflet primordium in wild-type plants (Wang et al., 2008) (Figure 1C), boundaries between lateral and terminal leaflet primordia failed to develop properly, resulting in leaflet fusion observed in *fcl1* mutants (Figures 1B and 1C).

In addition to the leaflet fusion phenotype, petiole development was also affected in the *fcl1* mutants. In 2-month-old plants, petioles developed on the youngest leaf (the first expanded leaf at the shoot apex) were normal in *fcl1* mutants, suggesting that the initial development of petioles was not affected in the mutants. However, petioles developed on the second and older leaves on the stem were significantly shorter in the *fcl1* mutants than the wild-type counterparts (Figures 1D and 1G). Since the average length of petiole epidermal cells was indistinguishable between *fcl1* mutants and wild-type plants, the reduced petiole elongation was not likely due to reduced cell elongation but instead may be due to compromised cell division activity in *fcl1* mutants (Figures 1E and 1F).

#### Molecular Cloning and Characterization of *FCL1*

To isolate the *FCL1* gene, we took a map-based approach. Genetic mapping results indicate that *FCL1* was closely linked to 12 simple sequence repeat (SSR) markers on chromosome 6 (see Supplemental Figure 1 online). To fine-map the *FCL1* locus, we generated a large F2 mapping population. Out of 787 F2 segregating plants, 213 plants were mutants and they were used to fine-map the *FCL1* locus (see Supplemental Table 1 online). Mapping results showed that the *FCL1* locus was flanked by two SSR markers, 005D01 and 002E12, and tightly linked to a newly developed SSR marker, AC141436-ssr4 (Figure 2A; see Supplemental Tables 2, 3, and 4 [for marker information] online). Using chromosomal walking and thermal asymmetric interlaced-PCR, we determined the deletion borders in both *fcl1-1* and *fcl1-2* mutants (Figures 2B and 2C; see Supplemental Figure 2 online). These results indicate that the region between coordinates 32,712 and 109,431 of the BAC clone AC141436 was deleted

*fcl1-1* (right) compound leaf primordia. Arrows indicate the boundary between terminal and lateral leaflet primordia developed at the P2 stage.

**(D)** Close-up views of mature leaves of the wild type (left) and the *fcl1-1* mutant (right), showing the reduced petiole in the mutant. Bar = 2 cm.

**(E)** Epidermal peels of petioles of compound leaves on the fourth node of 2-month-old wild type (left) and *fcl1-1* mutant (right).

**(F)** Measurements of petiole epidermal cell lengths of the wild type and the *fcl1-1* mutant. Shown are means  $\pm$  SD;  $n > 200$ .

**(G)** Measurements of petiole lengths of compound leaves at various developmental stages in 2-month-old wild type and *fcl1-1* mutant. Shown are means  $\pm$  SD;  $n = 10$ .

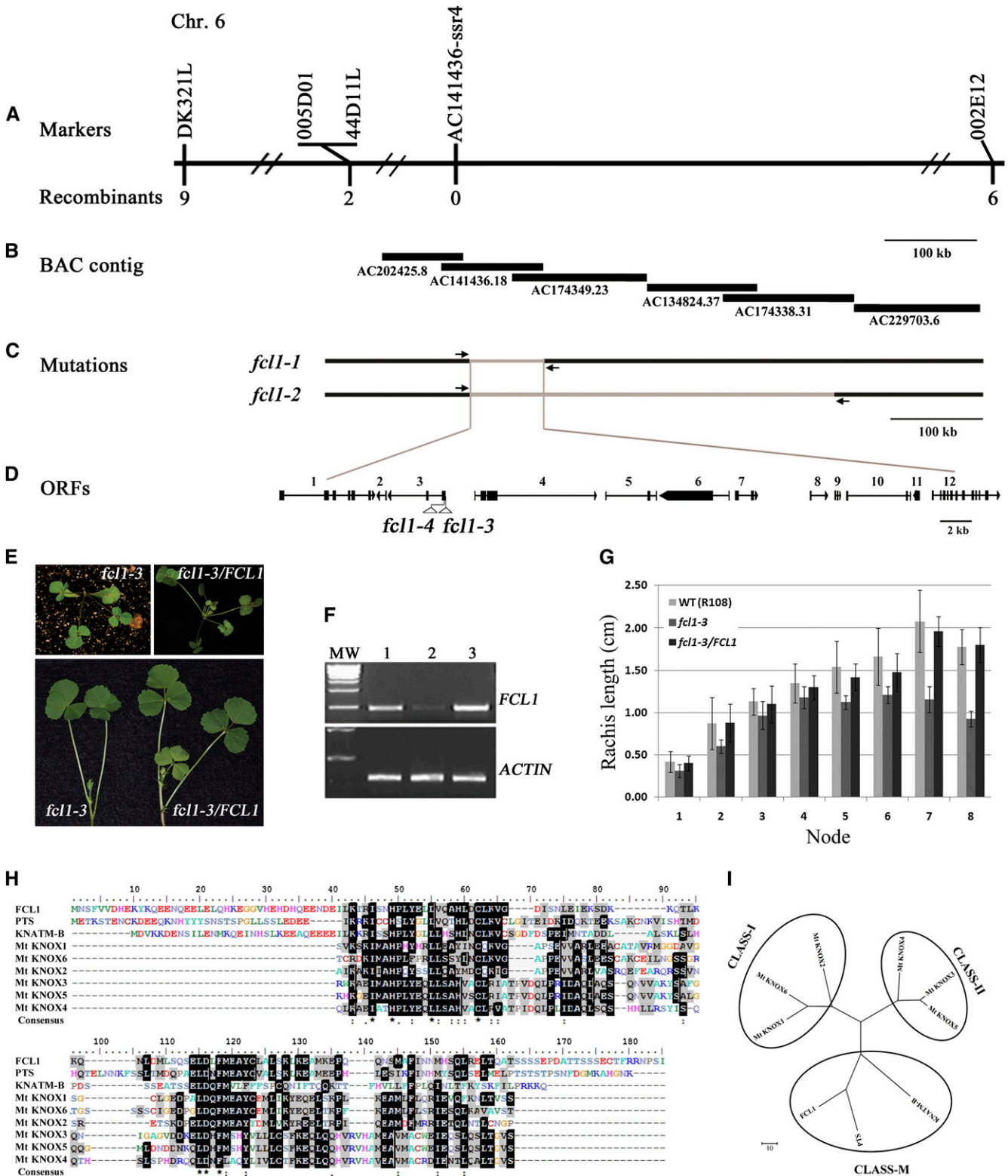


**Figure 2.** Map-Based Cloning of *FCL1*.

(A) The *FCL1* locus was mapped to the region between SSR markers 005D01 and 002E12 on chromosome (Chr.) 6. AC141436-SSR4, a newly developed SSR marker, cosegregated with *fc11*. The number of recombinants between markers and the *FCL1* locus is shown underneath the markers.

in both *fcl1-1* and *fcl1-2* (Figure 2C; see Supplemental Figure 2 online). Within this region are 12 annotated open reading frames (ORFs) (Figure 2D; see Supplemental Table 5 online). Using tissue-specific RT-PCR, the expression of six ORFs, *Medtr6g080670*, *Medtr6g080690*, *Medtr6g080700*, *Medtr6g080720*, *Medtr6g080770*, and *Medtr6g080780*, in the deletion region could be clearly detected in the vegetative shoot apices of wild-type plants (see Supplemental Figure 2B online).

To identify the *FCL1* gene from the set of 12 candidate genes deleted in both *fcl1-1* and *fcl1-2*, we first screened a tobacco (*Nicotiana tabacum*) *Tnt1* retrotransposon insertion mutant collection of *M. truncatula* (cv R108) (Tadege et al., 2008) and isolated one mutant with a weak leaflet fusion phenotype. Leaflets developed in the first three adult leaves were either fused to form simplified leaves or clustered without the rachis structure in the mutant (Figure 2E; see Supplemental Figure 3 online). Although leaflets in older leaves of the mutant were separated from each other, the length of rachis was significantly shorter in later developed leaves in the mutant than in the corresponding wild-type leaves (Figures 2E and 2G). F1 plants derived from genetic crosses between the third mutant and *fcl1-1* exhibit the weak leaflet fusion phenotype similar to the third mutant, confirming that it is a new *fcl1* allele (see Supplemental Figure 3 online). Accordingly, we named it *fcl1-3*. Flanking sequence analysis indicated that *fcl1-3* carries a tobacco *Tnt1* retrotransposon in the 5' untranslated region (UTR) of the third ORF in the deletion region, corresponding to *Medtr6g080690* (see Supplemental Figure 3 online). RT-PCR analysis indicated that the expression of *Medtr6g080690* was not abolished but was substantially reduced in *fcl1-3* compared with the corresponding wild type (cv R108) (Figure 2F). Thus, the reduced expression of *Medtr6g080690* is consistent with the weak leaflet fusion phenotype observed in this mutant.

Using a reverse genetic screen, we uncovered an additional allele, *fcl1-4*, with the *Tnt1* retrotransposon inserted in the first exon of *FCL1* (see Supplemental Figure 3 online). Mutant plants exhibit strong compound leaf phenotype similar to the deletion alleles *fcl1-1* and *fcl1-2* (see Supplemental Figures 3 and 4 online).

To further confirm the identity of *FCL1*, we performed genetic complementation tests. A 7.8-kb genomic sequence from wild-type plants (cv Jemalong A17), including 2664-bp 5' upstream sequence, 4242-bp coding region, and 1737-bp 3' downstream region, was stably introduced into both *fcl1-1* and *fcl1-3* mutants via *Agrobacterium tumefaciens*-mediated plant transformation. We show that this wild-type sequence complemented both *fcl1-1* and *fcl1-3* mutants (Figures 2E to 2G; see Supplemental Figure 5 online). Introducing ORF6, a putative zinc finger transcription factor gene, which is deleted in the *fcl1-1* and *fcl1-2* mutants, did not rescue the compound leaf phenotype of the *fcl1-1* mutant (see Supplemental Figure 6 online). Taken together, these results collectively confirm that the *FCL1* gene corresponds to *Medtr6g080690*.

### *M. truncatula* *FCL1* Encodes a Class M KNOX Protein

To identify the full-length transcript, we performed both 5'- and 3'-rapid amplification of cDNA ends (RACE). Sequence analysis indicates that only one full-length cDNA of 794 bp long was amplified, including a 99-bp 5'-UTR, 486-bp coding region, and 209-bp 3'-UTR (see Supplemental Figure 7 online). Comparison of genomic and cDNA sequences revealed that *FCL1* is composed of three exons and two introns. *FCL1* encodes a polypeptide of 161 amino acids.

BLAST analysis of the National Center for Biotechnology Information (NCBI) protein database (Altschul et al., 1997) revealed that *FCL1* encodes a truncated KNOX that contains both KNOX1 and KNOX2 domains (collectively called the MEINOX domain) but lacks the homeodomain (Figure 2H; see Supplemental Figure 7 online). Amino acid sequence comparison indicated that the *FCL1* protein shares a high sequence similarity with the *Arabidopsis* KNATM-B (63% similarities and 43% identities) and tomato PTS/TKD1 (60% similarities and 48% identities), two recently identified class M homeodomainless KNOX proteins in *Arabidopsis* and tomato, respectively (Kimura et al., 2008; Magnani and Hake, 2008) (Figure 2H). Neighbor-joining, maximum parsimony, and UPGMA phylogenetic tree

**Figure 2.** (continued).

**(B)** BAC contigs spanning the *FCL1* locus.

**(C)** Deletion borders identified in *fcl1-1* and *fcl1-2* alleles. Arrows represent primers used to amplify deletion junctions.

**(D)** Orientation and exon-intron structures of 12 annotated ORFs within the common deletion region in *fcl1-1* and *fcl1-2* alleles. Numbers above ORFs from 1 to 12 correspond to the following genes: 1, *Medtr6g080670*; 2, *Medtr6g080680*; 3, *Medtr6g080690*; 4, *Medtr6g080700*; 5, *Medtr6g080710*; 6, *Medtr6g080720*; 7, *Medtr6g080730*; 8, *Medtr6g080740*; 9, *Medtr6g080750*; 10, *Medtr6g080760*; 11, *Medtr6g080770*; and 12, *Medtr6g080780*. Solid boxes denote exons, and horizontal lines denote introns. Open triangles represent *Tnt1* insertion sites in ORF3 in *fcl1-3* and *fcl1-4* alleles.

**(E)** Genetic complementation of the *fcl1-3* mutant. Shown are 3-week-old *fcl1-3* mutant (top left), *fcl1-3* stably transformed with the full-length wild-type *FCL1* genomic sequence (top right), and compound leaves developed from leaf axils in 2-month-old plants (bottom left, *fcl1-3*; bottom right, *fcl1-3* complemented line).

**(F)** RT-PCR analysis of *FCL1* gene expression in the wild type, *fcl1-3*, and *fcl1-3* transformed with the wild-type *FCL1* gene. An *ACTIN* gene was used as an internal control.

**(G)** Measurements of rachis length of compound leaves of *fcl1-3* and *fcl1-3* transformed with the wild-type (WT) *FCL1* gene.

**(H)** Amino acid sequence alignments of the full-length *FCL1*, its close homologs from tomato and *Arabidopsis*, PTS and KNATM-B, respectively, and the MEINOX domains of six *M. truncatula* KNOX proteins.

**(I)** Neighbor-joining, maximum parsimony, and UPGMA phylogenetic tree analysis of *FCL1*, its close homologs from tomato and *Arabidopsis*, and the canonical KNOX proteins from *M. truncatula*.

[See online article for color version of this figure.]

analysis indicated that *FCL1* is grouped with *PTS/TKD1* and *KNATM-B* but separated from the canonical class I and class II *KNOX* proteins from *M. truncatula* (Figure 2I; see Supplemental Data Set 1 online). BLAST searches of genome sequences and subsequent sequence annotation further revealed the existence of homologous sequences in closely related species such as *L. japonicus* and soybean, other eudicot species such as poplar (*Populus trichocarpa*) and grape (*Vitis vinifera*), and monocot species such as rice (*Oryza sativa*) and maize (see Supplemental Figure 8 online). As expected, duplicated genes are present in the soybean and rice genomes due to whole-genome duplications in these species (see Supplemental Figure 8 online).

### Expression Pattern of *FCL1* and Subcellular Localization of the Encoded Protein

RT-PCR analyses revealed that *FCL1* is expressed in vegetative shoot apices, petioles, stems, roots, flowers, and seedpods with the highest level of expression being detected in roots and vegetative shoot buds (Figures 3A and 3B). The tissue-specific expression pattern is consistent with the microarray-based *in silico* analysis of *FCL1* expression (Benedito et al., 2008) (see Supplemental Figure 9 online).

RNA *in situ* hybridization was performed to examine tissue- and cell-specific expression patterns of *FCL1* in vegetative shoot apices. We show that *FCL1* transcripts were detected in leaf primordia at P0 and early P1 stages (Figures 3C and 3E, arrows). At later stages, *FCL1* transcripts were detected at boundaries between leaf primordia and the SAM and at the proximal adaxial domain of developing leaf primordia (Figures 3C and 3E, arrowheads), which is the future site of the petiole. In addition, RNA *in situ* hybridization results show that *FCL1* transcripts were not detected in the SAM (Figures 3C and 3E). As a negative control, a sense probe did not give any signal (Figure 3D).

To confirm and further investigate *FCL1* expression pattern, we introduced an *FCL1* promoter:*uidA* reporter gene construct into wild-type *M. truncatula* plants (cv R108) via *A. tumefaciens*-mediated stable plant transformation. We show that the reporter gene expression was detected in the root, cotyledon, petiole, rachis, and young developing leaves in homozygous T3 plants (Figures 3F and 3G). In developing leaves, the reporter gene was weakly expressed in vascular tissues.

The *FCL1* protein does not contain any known subcellular localization signals. To determine *FCL1* subcellular localization, we transiently expressed *FCL1* fused to the green fluorescent protein (*FCL1-GFP*) under control of the constitutive cauliflower mosaic virus 35S promoter in tobacco leaves. The *FCL1-GFP* fusion protein was detected in both cytoplasm and nucleus in tobacco epidermal cells similarly to the localization pattern of free GFP (35S:GFP) (Figures 3H and 3I). The subcellular localization pattern suggests that *FCL1* may move freely between nucleus and cytoplasm likely due to its small size.

### Expression of Class I *KNOX* Genes Was Not Altered in Loss-of-Function *fcl1* Mutants

Previous studies have shown that class I *KNOX* proteins are not detectable in compound leaf primordia in IRLC legumes

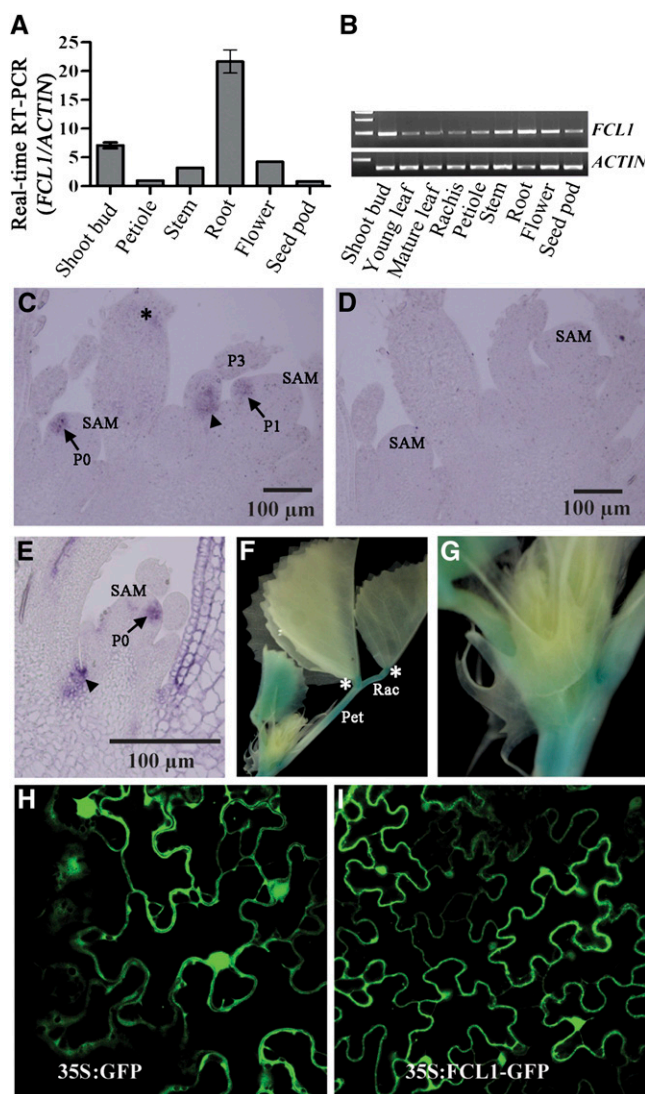


**Figure 3.** Tissue-Specific Expression of *FCL1* and Subcellular Localization of the Encoded Protein.

(A) and (B) RT-PCR analysis of tissue-specific expression of *FCL1*. (C) to (E) RNA *in situ* hybridization analysis of *FCL1* expression in vegetative shoot buds. A sense probe was used as a negative control (D). (F) and (G) *FCL1* promoter:*GUS* reporter gene expression in shoot apices in stable transgenic lines. (H) Subcellular localization of 35S:GFP in tobacco epidermal cells. (I) Subcellular localization of 35S:*FCL1-GFP* in tobacco epidermal cells. P, plastochron; Pet, petiole; Rac, rachis. Arrowheads in (C) and (E) indicate proximal adaxial domain, and asterisks in (C) and (F) indicate the petiole.

(Champagne et al., 2007). To test whether loss-of-function mutations in *FCL1* affect spatial-temporal expression of class I *KNOX* genes in *M. truncatula*, we examined expression of three class I *KNOX* genes, *KNOX1*, *KNOX2*, and *KNOX6*, in the *fcl1-1* mutant. Real-time RT-PCR analysis indicated that *KNOX1*,

*KNOX2*, and *KNOX6* were similarly expressed in the vegetative shoot buds in the wild type and *fc1-1* mutant (Figure 4A; see Supplemental Figures 10A and 10B online). Also, their expression was similarly diminished in young leaves in the wild type and *fc1-1* mutant (Figure 4A; see Supplemental Figures 10A and 10B online). RNA in situ hybridization analysis indicated that *KNOX1* transcripts were present in the SAM but excluded from incipient and subsequent leaf primordia in both the wild type and *fc1-1* mutant (Figures 4B and 4C), consistent with the quantitative RT-PCR results and with previous studies. As a negative control, a sense probe did not detect any signals (Figure 4D). These results indicate that *FCL1* does not appear to regulate temporal-spatial expression of class I *KNOX* genes in *M. truncatula*.

### FCL-BELL and FCL-KNOX Protein Interactions

*Arabidopsis* KNATM-B contains a full MEINOX domain and has been shown to interact with the homeodomain BELL proteins, including BEL1, SAW1, SAW2, and PNY, but not the PNY paralog PNF (Magnani and Hake, 2008). The *M. truncatula* FCL1 is predicted to contain an intact MEINOX domain (Figure 2H; see Supplemental Figure 7 online). To investigate whether FCL1 interacts similarly as KNATM-B, we performed yeast two-hybrid assays using FCL1 as the bait and *Arabidopsis* BELL proteins as preys. To our surprise, unlike KNATM-B, which activates reporter gene expression by itself in the yeast two-hybrid assays (Magnani and Hake, 2008), FCL1 did not activate reporter gene expression by itself (Figures 5A and 5B). Furthermore, we ob-

served that FCL1 strongly interacted with a subset of the BELL proteins, including PNY, SAW1, and BEL1, but not with SAW2 and PNF (Figures 5A and 5B). These interactions were further confirmed by quantification of the reporter gene expression in yeast (Figure 5B). Thus, FCL1 interacts with BELL proteins with slightly different specificities compared with the *Arabidopsis* KNATM-B. Interestingly, both FCL1 and KNATM-B did not interact with PNF, the PNY paralog (Magnani and Hake, 2008) (Figures 5A and 5B).

KNATM-B has been shown to interact strongly with BP/KNAT1 and weakly with KNAT3 and KNAT4 in the yeast two-hybrid assays (Magnani and Hake, 2008). By contrast, FCL1 did not interact with BP/KNAT1 and other KNOX proteins from *Arabidopsis* (Figure 5). We also tested FCL1 interactions with KNOX proteins from *M. truncatula*. We show that FCL1 did not interact with the *M. truncatula* KNOX proteins in the yeast two-hybrid assays. Although we observed weak X-gal staining from interactions between FCL1 and *M. truncatula* KNOX3 and KNOX4 in a prolonged incubation, quantification results suggest that the reporter gene expression was only slightly above the background level (Figure 5B). In addition, FCL1 did not interact with itself, KNATM-B, SGL1, or PALM1 (Figure 5).

### Genetic Interactions between *fc1* and *sgl1*

Our genetic analysis suggests that *FCL1* is required for the development of boundaries between terminal and lateral leaflet primordia at the P2 stage and development of petioles at a later stage during compound leaf development in *M. truncatula*

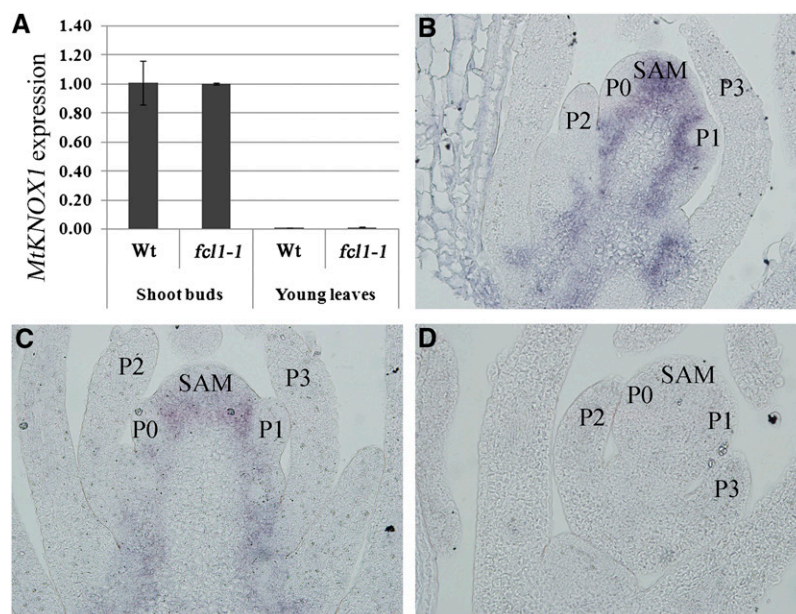


**Figure 4.** *KNOX1* Expression in the *fc1-1* Mutant.

**(A)** Real-time RT-PCR analysis of *KNOX1* expression in vegetative shoot buds and young leaves in the wild type (Wt) and *fc1-1* mutant. An *M. truncatula* *ACTIN* gene was used as an internal control.

**(B)** and **(C)** RNA in situ hybridization analysis of *KNOX1* expression in shoot apices of the wild type **(B)** and *fc1-1* mutant **(C)**.

**(D)** A negative control for RNA in situ hybridization using a sense probe and an adjacent section of shoot apices of the *fc1-1* mutant. P, plastochron.

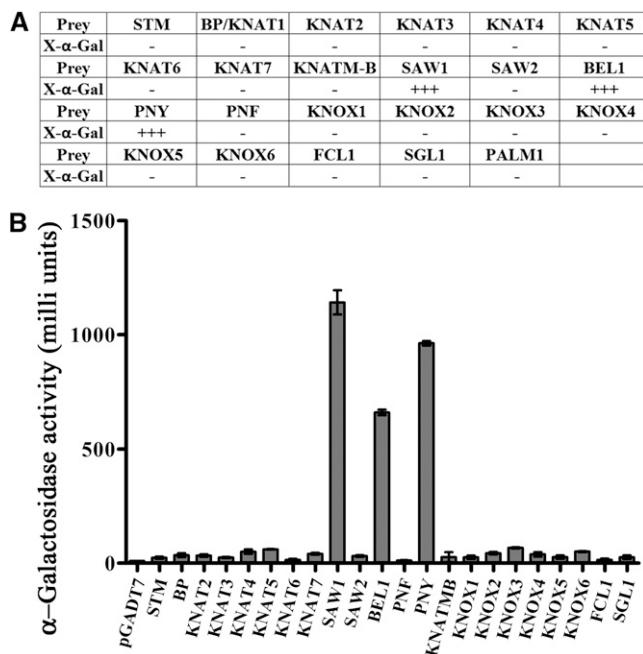


**Figure 5.** Yeast Two-Hybrid Assays for Protein–Protein Interactions.

(A) X- $\alpha$ -gal activity staining for protein–protein interactions between FCL1 and the following proteins: STM, BP/KNAT1,KNAT2, KNAT3, KNAT4, KNAT5, KNAT6, KNAT7, KNATM-B, SAW1, SAW2, BEL1, PNF, PNY, KNOX1, KNOX2, KNOX3, KNOX4, KNOX5, KNOX6, FCL1, SGL1, and PALM1.

(B) Quantification of protein–protein interactions. Shown are means  $\pm$  SD;  $n = 3$ .

(Figure 1). Previously, we have shown that *SGL1*, the *M. truncatula* *FLO/LFY/UNI* ortholog, is required for the initiation of lateral leaflet primordia and development of petioles (Wang et al., 2008). The involvement of *SGL1* in petiole development appears to be similar to that of *FCL1*. To examine genetic interactions between *fcl1* and *sgl1*, we made crosses between *sgl1-1* and *fcl1-1* and generated *sgl1 fcl1* double mutants (see Supplemental Table 6 online). Mature leaves of *sgl1 fcl1* double mutants were simple, resembling those of *sgl1* mutants (Figures 6A and 6B). Flowers developed in the double mutants also resembled those of *sgl1* mutants (Figure 6C). These results indicate that *sgl1* is genetically epistatic to *fcl1* in both leaf patterning and flower development. By contrast, both *sgl1* and *fcl1* had about a 50% reduction in petiole length compared with their wild-type counterparts, and *sgl1 fcl1* double mutants completely lacked petioles (Figures 6A, 6B, and 6D), suggesting that *SGL1* and *FCL1* act additively and both are required for petiole development. Since there were no significant differences in epidermal cell length of petioles between the wild type and *sgl1* mutants (Figures 6E and 6F), the reduced petiole development in *sgl1* mutants is likely due to reduced cell division as in *fcl1* mutants (Figures 1D to 1G). RT-PCR analysis of *sgl1* and *fcl1* mutants suggests that *SGL1* and *FCL1* do not appear to regulate each other's transcript levels (Figures 7B and 7D). In addition, *SGL1*

and *FCL1* did not interact with each other in the yeast two-hybrid assays (Figure 5).

### Genetic Interactions between *fcl1* and *palm1*

Another key regulator of compound leaf development in *M. truncatula* is the recently identified *PALM1* gene, which encodes a Cys(2)His(2) zinc finger transcription factor (Chen et al., 2010; Ge et al., 2010). Mature leaves of loss-of-function *palm1* mutants are pentafoliolate with longer petioles, in contrast with trifoliolate wild-type leaves (Chen et al., 2010) (Figure 7A). To investigate genetic interactions between *fcl1* and *palm1*, we generated *fcl1 palm1* double mutants (see Supplemental Table 6 online). The *fcl1 palm1* double mutants exhibited fused compound leaves and short petioles, resembling those of *fcl1* mutants (Figures 7A and 7C). These results indicate that *fcl1* is genetically epistatic to *palm1* in both leaf complexity and petiole development. Previous studies have shown that the increase in leaflet number and petiole elongation is attributed to a significantly increased level of *SGL1* expression in *palm1* mutants (Chen et al., 2010) (Figures 7B and 7D). We show that the increase in *SGL1* expression was not affected in the *fcl1 palm1* double mutants (Figures 7B, 7D, and 8). Interestingly, despite an increase in *SGL1* expression, *fcl1 palm1* double mutants did not produce extra leaflets (Figures 7A and 8). In loss-of-function *fcl1* mutants, the *PALM1* transcript level was not altered as indicated by RT-PCR data (Figures 7B and 7D). Although these results suggest no direct transcriptional regulation of *PALM1* by *FCL1*, it is still possible that subtle or tissue-specific differences in *PALM1* expression might occur but were not detected in *fcl1* mutants due to limitations of RT-PCR. Our data also show that *FCL1* and *PALM1* did not interact in yeast two-hybrid assays (Figure 5). Taken together, these results suggest that, although *FCL1* is not required for the upregulation of *SGL1* expression in the loss-of-function *palm1* mutants, it is required for the development of extra leaflet primordia in the absence of the *PALM1* gene (Figure 8).

## DISCUSSION

Phylogenetic analysis of leaf evolution suggests that compound leaves arose numerous times from the ancestral form, during the evolution of angiosperms (Bharathan et al., 2002; Champagne and Sinha, 2004). Consistent with this, recent molecular genetic studies demonstrate that *KNOX1*- and *UNI/SGL1*-dependent processes are required for compound leaf development in most compound-leaved species, including tomato and legume species belonging to the IRLC. In some legume species with compound leaves, *KNOX1* transcripts and encoded proteins are excluded from the incipient and developing leaf primordia, supporting that they are not associated with compound leaf development in these legume species. Interestingly, developmental programs are still responsive to ectopic expression of *KNOX1* genes in legumes, consistent with the notion that *UNI/SGL1* transcription factors are recruited to function in place of *KNOX1* proteins in compound leaf development in IRLC legumes. However, molecular mechanisms of compound leaf development in legumes remain to be elucidated.



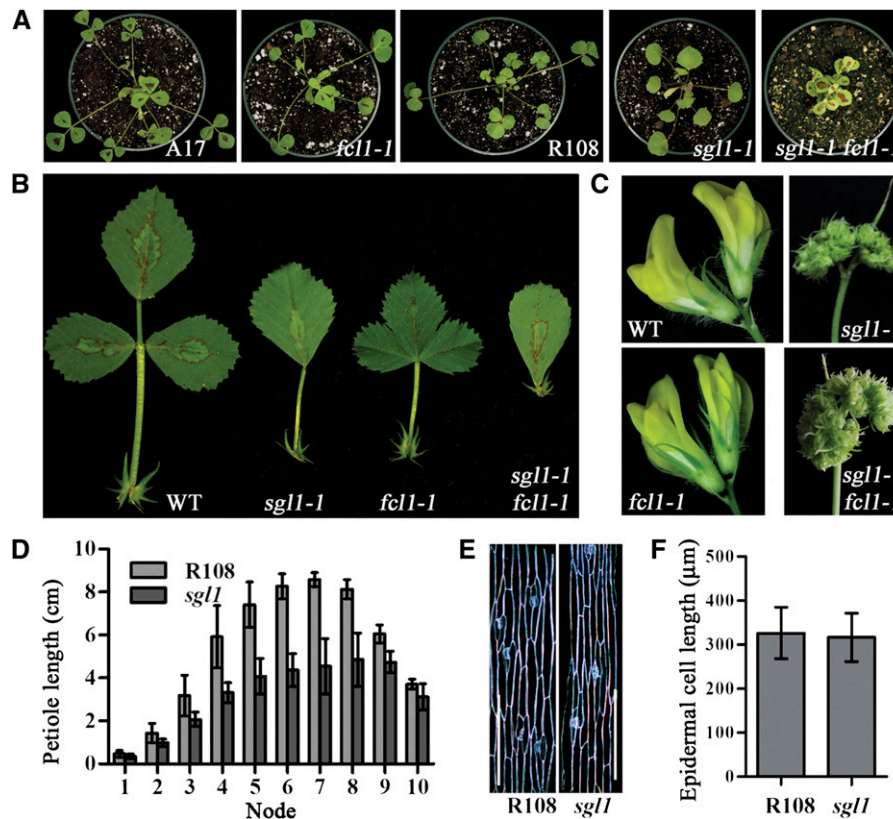


**Figure 6.** Genetic Interactions between *fcl1* and *sgl1*.

- (A) Three-week-old seedlings (from left to right: Jemalong A17, *fcl1-1*, R108, *sgl1-1*, and *sgl1 fcl1* plants).  
 (B) Comparison of compound leaf morphology (from left to right: Jemalong A17, *sgl1-1*, *fcl1-1*, and *sgl1-1 fcl1-1*). WT, wild type.  
 (C) Comparison of flower morphology (clockwise from top left: Jemalong A17, *sgl1-1*, *sgl1-1 fcl1-1*, and *fcl1-1*).  
 (D) Measurements of petiole lengths of the wild type (R108) and *sgl1-1*. Shown are means  $\pm$  SD;  $n = 10$ .  
 (E) Epidermal peels of petioles in the wild type (R108; left) and *sgl1-1* mutant (right).  
 (F) Measurements of epidermal cell lengths of petioles in the wild type (R108) and *sgl1-1* mutant. Shown are means  $\pm$  SD;  $n > 200$ .  
 [See online article for color version of this figure.]

Here, we report isolation of two deletion mutants in *M. truncatula*, in which *FCL1* is completely deleted, and two insertion mutants, in which *FCL1* expression is partially or completely compromised. Loss-of-function *fcl1* mutants exhibit various compound leaf defects, ranging from leaflet fusion to simple leaves and leaflet clustering. In addition to leaflet patterning defects, petiole elongation is also affected in *fcl1* mutants. In the partial loss-of-function *fcl1* mutant (*fcl1-3*), compound leaf development is only mildly affected. In the first three adult leaves developed on the main stem and from axils of primary leaves, leaflets lack rachis and are clustered. Although leaflets of later developed leaves are separated from each other, the length of both rachis and petiole is significantly reduced in the weak *fcl1-3* mutant compared with the wild type. The effect of *FCL1* on compound leaf development suggests that *FCL1* plays two distinct roles in compound leaf development (i.e., boundary separation of leaflet primordia at the P2 stage and the proximal-distal axis development at later stages [after P4]). Because the petiole epidermal cell length is not affected, the reduced petiole

development in *fcl1* mutants is likely due to a compromised cell division activity but not cell elongation. We hypothesize that *FCL1* is required to maintain windows of organogenetic activities at the leaf margin at an early stage for boundary separation and at a later stage for petiole development. Mutations in *FCL1* shorten the windows of organogenetic activities and promote leaf maturation, leading to clustering and fusion of leaflets, simple leaves, and reduced petiole development. This hypothesis is supported by genetic analyses of two other compound leaf mutants. Loss-of-function *sgl1* mutants exhibit simple leaves and reduced petioles, and loss-of-function *palm1* mutants exhibit an increased level of *SGL1* gene expression and proliferation of leaflets and increased petioles (Wang et al., 2008; Chen et al., 2010) (Figure 8). During early stages of leaf development, *SGL1* is epistatic to *FCL1*, highlighting a requirement for *SGL1* in the development of trifoliolate compound leaves (Figure 8). During later stages of leaf development, *SGL1* and *FCL1* are involved in separate processes and both are required for petiole development (Figure 8). Previous studies suggest that the proliferation of

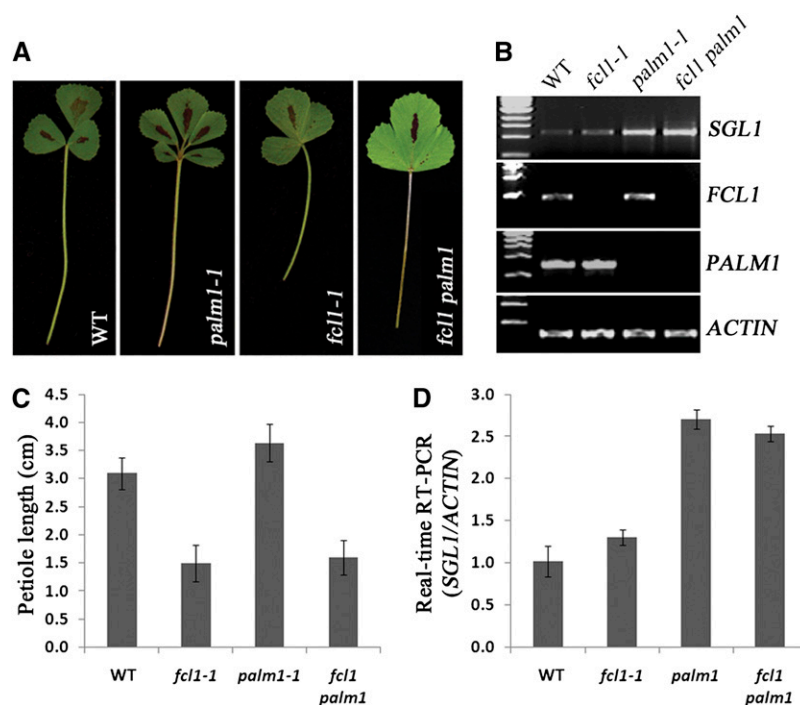


**Figure 7.** Genetic Interactions between *fcl1* and *palm1*.

(A) Compound leaf morphology (from left to right: Jemalong A17, *palm1-1*, *fcl1-1*, and *fcl1-1 palm1-1*). WT, wild type.

(B) RT-PCR analysis of *SGL1*, *FCL1*, *PALM1*, and *ACTIN* gene expression in vegetative shoot buds of the wild type (Jemalong A17), *fcl1-1*, *palm1-1*, and *fcl1-1 palm1-1* mutants.

(C) Measurements of petiole length of the wild type (Jemalong A17), *fcl1-1*, *palm1-1*, and *fcl1-1 palm1-1* mutants.

(D) Real-time RT-PCR analysis of *SGL1* expression in the wild type (Jemalong A17), *fcl1-1*, *palm1-1*, and *fcl1-1 palm1-1* mutants. Shown are means  $\pm$  SD;  $n = 3$ .

[See online article for color version of this figure.]

compound leaves in *palm1* mutants is attributed to an increase in *SGL1* expression (Chen et al., 2010). However, our double mutant analyses indicate that an increase in *SGL1* gene expression alone is not sufficient for the proliferation of compound leaves in *palm1* mutants. Instead, both *SGL1* and *FCL1* are required for the development of pentafoliolate leaves in the absence of *PALM1*. The results are consistent with a role of *FCL1* in maintaining windows of organogenetic activities at the leaf margin required for compound leaf development in *M. truncatula*.

*FCL1* encodes a truncated KNOX that contains both KNOX1 and KNOX2 domains (collectively called the MEINOX domain) but lacks the homeodomain. Phylogenetic analysis indicates that *FCL1* is a member of the class M KNOX proteins, including two recently identified members from tomato and *Arabidopsis*, PTS/TKD1 and KNATM-B, respectively. The function of PTS/TKD1 and KNATM-B needs to be further elucidated because no loss-of-function mutants of these two genes have been isolated so far. Nonetheless, ectopic expression of KNATM-B results in elongated petioles and narrower, shorter, and serrated leaves in *Arabidopsis* (Magnani and Hake, 2008). In tomato plants, the semidominant *Petroselinum* (*Pts*) mutant, caused by upregulation of *PTS/TKD1* due to mutations in its promoter region, exhibits a proliferation of compound leaves, affecting both

primary and secondary leaflets (Kimura et al., 2008). The gain-of-function phenotypes in *Arabidopsis* with simple leaves and tomato with compound leaves are consistent with expected results from compound leaf defects of the loss-of-function *M. truncatula fcl1* mutants. Taken together, these observations support a general role of the class M KNOX proteins in the development of both simple and compound leaves in diverse species.

The *fcl1-1* and *fcl1-2* mutant alleles derived from fast neutron bombardment mutagenesis carry a common deletion of  $\sim 77$  kb on chromosome 6. Commonly deleted in *fcl1-1* and *fcl1-2* alleles are 12 putative genes, six of which are expressed in vegetative shoot buds and possibly play a role in shoot development. In this study, we showed that *FCL1* plays important roles in compound leaf development. Interestingly, one of the deleted genes, *Medtr6g080720*, is also expressed in the shoot apices and encodes a putative zinc finger domain transcription factor that belongs to the highly conserved human NF-X1 family of transcription factors. Although our data indicate that *Medtr6g080720* is not involved in compound leaf development, previous studies have shown that the two *Arabidopsis* homologs, *NFXL1* and *NFXL2*, play antagonistic roles in abiotic and biotic stress responses in plants (Lisso et al., 2006; Asano et al., 2008). It would

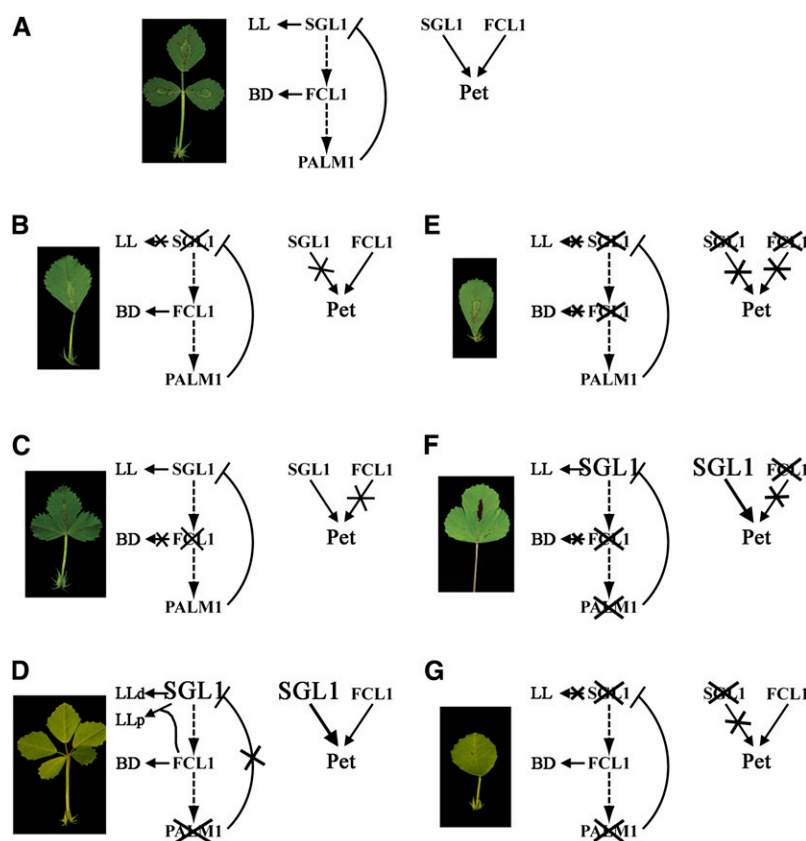


**Figure 8.** A Genetic Model of Compound Leaf Development in *M. truncatula*.

**(A)** Wild-type *M. truncatula* plants exhibit trifoliolate compound leaves. Double mutant analyses indicate that *sgl1* is epistatic to *fcl1*, and *fcl1* is epistatic to *palm1* in terms of leaf complexity (dashed arrows; also see below). In terms of leaf proximal-distal axis development, *SGL1* and *FCL1* are additive (arrows). It has been shown that *PALM1* represses *SGL1* transcription by directly binding to its promoter sequence (Chen et al., 2010). Together, *SGL1*, *FCL1*, and *PALM1* define the trifoliolate morphology of wild-type leaves. BD, boundary between terminal and lateral leaflet primordia; LL, lateral leaflet primordia; Pet, petiole.

**(B)** Loss-of-function mutations in *SGL1* result in plants with simple leaves and reduced petioles, consistent with its role in the initiation of lateral leaflet primordia at an early stage and the leaf proximal-distal axis development at a late stage (Wang et al., 2008).

**(C)** Loss-of-function mutations in *FCL1* result in fusion of leaflets and reduced petioles, consistent with its role in boundary separation and the proximal-distal axis development (this study).

**(D)** Loss-of-function mutations in *PALM1* results in proliferation of compound leaves and slightly elongated petioles. In *palm1* mutants, the *SGL1* transcript level is significantly increased, consistent with its negative role in transcriptional regulation of *SGL1* expression in wild-type plants (Chen et al., 2010).

**(E)** The *sgl1 fcl1* double mutants exhibit simple leaves, indicating that *sgl1* is epistatic to *fcl1* in terms of leaf complexities. *sgl1* and *fcl1* single mutants have ~50% reduction in petiole length, and *sgl1 fcl1* double mutants completely lack petioles, indicating an additive interaction between *SGL1* and *FCL1* in leaf proximal-distal axis development.

**(F)** The *fcl1 palm1* double mutants exhibit leaflet fusion similar to the *fcl1* mutants, indicating that *fcl1* is epistatic to *palm1* (this study). Interestingly, in *fcl1 palm1* double mutants, the *SGL1* transcript level is still significantly increased but no extra leaflets are developed, suggesting that *FCL1* is not required for the upregulation of *SGL1* but required for the development of extra leaflets in *palm1* single mutants (this study).

**(G)** The *sgl1 palm1* double mutants exhibit simple leaves with reduced petioles similarly as the *sgl1* single mutants, indicating that *sgl1* is epistatic to *palm1* (Chen et al., 2010).

[See online article for color version of this figure.]

be interesting to test whether *Medtr6g080720* plays a similar role as its *Arabidopsis* homolog does.

How class M KNOX proteins regulate leaf development remains to be elucidated. It has been shown that KNATM-B and PTS/TKD1 form heterodimers with BELL proteins (Kimura et al., 2008; Magnani and Hake, 2008). The *Arabidopsis* BELL proteins

SAW1 and SAW2 interact with the canonical KNOX1 proteins and act redundantly to repress *KNOX* expression in leaves (Kumar et al., 2007). Through interactions with the BELL protein BIPIN-NATA (BIP), PTS/TKD1 antagonizes BIP and KNOX1 interactions and interferes with BELL and KNOX regulatory networks (Kimura et al., 2008). In a large number of compound-leafed legume

plants that belong to the IRLC, KNOX1 proteins are permanently downregulated in leaf primordia and are likely not associated with compound leaf development in these species (Champagne et al., 2007). The involvement of a truncated KNOX protein (FCL1) in compound leaf development in *M. truncatula*, an IRLC legume, is surprising and poses an interesting question of the role of *FCL1* in compound leaf development. Although further investigation is required to understand the role of *FCL1* in compound leaf development, we have shown that FCL1 selectively interacts with a subset of BELL proteins, including SAW1, BEL1, and PNY, but not with SAW2 and PNF in yeast two-hybrid assays. In *Arabidopsis*, *SAW1* and *BEL1* transcripts can be detected in developing leaves (Kumar et al., 2007). It is possible that *M. truncatula* *SAW1* and *BEL1* homologs are also expressed in leaves and play a role in compound leaf development through interactions with FCL1. The selectivity of FCL1 interactions with BELL proteins is slightly different from KNATM-B since the latter strongly interacts with SAW2 (Magnani and Hake, 2008). In addition, unlike KNATM-B, FCL1 does not interact with the KNOX1 protein, BP/KNAT1. RNA in situ hybridization results indicate that *FCL1* is expressed in the incipient leaf primordia (P0) but not in the SAM. Thus, *FCL1* expression appears not to overlap with that of *KNOX1* genes in *M. truncatula*. These results, together with others, collectively suggest that *FCL1* may regulate compound leaf developmental processes through specific protein-protein interactions with BEL1-like homeodomain proteins. Alternately, FCL1 may be involved in regulating NAM/CUC transcription factor-dependent and/or auxin transport-dependent regulatory networks known to be required for boundary separation and various developmental processes in diverse species. Future investigation will be aimed at elucidating the regulatory roles of the class M KNOX protein in leaf development in legume.

## METHODS

### Plant Materials

Seeds of *Medicago truncatula* cv Jemalong A17 were exposed to fast neutron radiation at the dosage level of 40 gray and germinated in a greenhouse with a controlled environment. Approximately 30,000 M2 plants derived from 5000 M1 lines were screened, resulting in the isolation of *fc1-1* (M368) and *fc1-2* (M602). The *fc1-3* and *fc1-4* alleles were isolated from a collection of tobacco (*Nicotiana tabacum*) *Tnt1* retrotransposon insertion mutants as previously described (Wang et al., 2008; Chen et al., 2010; Cheng et al., 2011). *fc1-1* was backcrossed to the parental line (cv Jemalong A17) for two generations. BC2 plants were used for phenotypic characterization. *fc1-2* was backcrossed to the Jemalong A17 line for four generations. BC4 plants were used.

### Scanning Electron Microscopy

Shoot apices of 2- to 4-week-old seedlings were subjected to vacuum infiltration in a fixative solution (3% glutaraldehyde in 25 mM phosphate buffer, pH 7.0) for 1 h and then incubated at 4°C overnight. Plant tissues were further fixed with 1.0% osmium tetroxide in the same phosphate buffer overnight and dehydrated in a graded ethanol series. Scanning electron microscopy was performed as described previously (Wang et al., 2008).

### Genetic Mapping

F2 mapping populations were generated from crosses between *fc1-2* and a polymorphic ecotype, *M. truncatula* cv Jemalong A20. Initially, an F2 population of 254 individuals (175 wild-type-like and 79 mutants; see Supplemental Table 1 online) was used in a bulk segregant analysis to construct a linkage map of the *fc1* locus. A total of 267 SSR markers distributed across the eight chromosomes of *M. truncatula* (<http://www.medicagohapmap.org/?genome>) were used to construct the linkage map. Subsequently, an F2 population of 533 individuals (399 wild-type-like and 134 mutants; Supplemental Table 1 online) was generated. A total of 213 *fc1* mutants were used to fine map the *FCL1* locus. Total genomic DNA was isolated from leaf tissues of individual plants grown in a greenhouse using a protocol previously described (Saghai-Marooof et al., 1984). PCR amplification and product separation were performed as previously described (Yu et al., 2006).

For genetic mapping, we made four DNA bulks, two from 15 wild-type plants each and two from 15 *fc1-1* mutant plants each by pooling equal amounts of DNA samples prepared from individual F2 plants. DNA samples from the two wild-type parental lines *M. truncatula* cv Jemalong A17 and Jemalong A20 were also included in the analysis to validate the markers.

Recombination frequency was calculated using the maximum likelihood estimator,  $P = (h + 2b)/2n$ , where  $P$  is the recombination frequency,  $n$  is homozygous recessive individuals in F2,  $h$  is the number of recombinant homozygotes, and  $b$  is the number of recombinant heterozygotes (Allard, 1956; Hinze et al., 1991). The Kosambi mapping function was used to estimate genetic distances between markers and the *fc1-2* locus as previously described (Koorneef et al., 1983). We constructed the linkage map using JoinMap (v3.0) (van Ooijen and Voorrips, 2001). For chromosomal walking, we designed PCR primers based on BAC sequences in the mapped region using Primer3 (Rozen and Skaletsky, 2000).

Bulked segregant analysis revealed that 12 of the 267 SSR markers located on chromosome 6 are cosegregated with the *fc1-2* locus. To construct a linkage map, we determined recombination frequencies and map positions for the 12 SSR markers using 254 individuals from an F2 mapping population. Based on this analysis, the *fc1-2* locus was mapped to the vicinity of four SSR markers, Mitc250, 005D01, 002E12, and 002F12, on chromosome 6 (see Supplemental Figure 1A online).

To fine-map the *fc1-2* locus, we examined a total of 213 *fc1-2* mutant plants identified from two F2 mapping populations of 787 individuals using the following SSR markers located in the region covered by three BAC clones (AC174349, AC141436, and AC202465) on chromosome 6: DK321L, 44D11L, 005D01, 002E12, 002F12, 18A5R, 19O4L, and AC141436-ssr4 (see Supplemental Tables 2 and 3 and Supplemental Figures 1B and 2 online). AC141436-SSR4 was designed based on the BAC clone AC141436 (see Supplemental Table 4 online).

Twenty mutant plants were identified carrying recombination between the parental Jemalong A20 allele and the *fc1-2* locus (see Supplemental Table 3 online). Two plants carried both parental alleles of the SSR markers 44D11L and 005D01, and six plants carried both parental alleles of the SSR marker 002E12 (see Supplemental Table 3 online; highlighted in red). These results indicate that two recombination events occurred between 44D11L and *fc1-2*, and 005D01 and *fc1-2*, and six recombination events occurred between 002E12 and *fc1-2*. In addition, these eight individuals only carried the mutant allele of the AC141436-ssr4 marker. These fine-mapping results indicate that the *fc1-2* locus was likely located within the BAC clone AC141436 and tightly linked to the SSR marker AC141436-ssr4 (see Supplemental Figure 1B online).

To delineate deletion borders, we initiated chromosomal walking. PCR primers were designed to scan the region covered by BAC clones AC174349, AC141436, and AC202465 of chromosome 6 (see Supplemental Table 4 online). Regular PCR and thermal asymmetric

interlaced-PCR amplifications and subsequent sequencing of deletion junctions indicate that the deletion in the *fc1-1* allele (M368) occurred within an ~80-kb interval between the coordinates 29,233 and 109,431 of the BAC clone AC141436, and the deletion in the *fc1-2* allele (M602) occurred within a large genomic interval starting from the coordinate 32,712 of the BAC clone AC141436 and ending in the BAC clone AC174338 (see Supplemental Figure 2 online). Thus, a genomic interval of ~76 kb between 32,712 and 109,431 of the BAC clone AC141436 was deleted in both the *fc1-1* and *fc1-2* alleles.

#### 5'- and 3'-RACE, RT-PCR, and Real-Time RT-PCR

Total RNA was prepared using the RNeasy plant mini kit (Qiagen). Residual genomic DNA was removed using a DNA-free kit (Ambion). The 5'- or 3'-RACE was performed using an RLM-RACE kit (Invitrogen) according to the manufacturer's instructions. cDNA synthesis for RT-PCR and real-time RT-PCR was performed using SuperScript III reverse transcriptase (Invitrogen) starting with 2 µg of total RNA in a 20-µL reaction mix with oligo(dT)<sub>15</sub> primer (Promega). Real-time RT-PCR was performed as previously described (Laxmi et al., 2008). Real-time RT-PCR was performed using a 7900HT Fast real-time PCR system (Applied Biosystems). SDS2.2.1 software (Applied Biosystems) was used to analyze the melt curve to confirm the single amplification. PCR efficiency was estimated using the LinRegPCR program (Ramakers et al., 2003), and the transcript level was determined in reference to the expression of the *M. truncatula* ACTIN gene (Medtr3g095530).

#### Genetic Complementation of *M. truncatula* *fc1* Mutants

The BAC clone AC141436 was digested with *Hind*III to generate a 7.8-kb genomic DNA fragment, which was subsequently ligated to *Hind*III-digested pCAMBIA3300 vector (CAMBIA). The final construct designated as pFCL1:FCL1 was sequenced to confirm no sequence errors. The construct was introduced into the *Agrobacterium tumefaciens* EHA105 strain using electroporation. The *fc1-1* and *fc1-3* alleles were transformed following the protocol previously reported (Cosson et al., 2006).

#### Epidermal Cell Length Measurement

Epidermal peels were made from the petiole of the fifth compound leaf of 2-month-old R108, *sgl1-1*, Jemalong A17, and *fc1-1* plants. More than 200 epidermal cells from multiple independent plants of each genotype were measured using Image J. Student's *t* tests were used for statistical analysis.

#### RNA in Situ Hybridization

RNA in situ hybridization was performed as previously described (Coen et al., 1990) with minor modifications. Briefly, *FCL1* and *KNOX1* transcripts were transcribed from cDNA clones corresponding to the nucleotide sequences from 60 to 459 and from 60 to 498 downstream of the translation initiation codon ATG of *FCL1* and *KNOX1*, respectively, and labeled with digoxigenin. Ten-micrometer sections from shoot apices of 2-week-old wild-type Jemalong A17 and *fc1-1* mutant were hybridized with the digoxigenin-labeled sense or antisense probes. Primer sequences used are listed in Supplemental Table 4 online.

#### Histochemical Analysis of the GUS Reporter Gene Expression

GUS activity staining was performed as previously described (Jefferson et al., 1987). Briefly, shoot buds were incubated in a GUS staining solution (100 mM sodium phosphate, pH 7.0, 1 mM EDTA, 0.05% Triton X-100, 1 mM potassium ferricyanide and potassium ferrocyanide, and 1 mg/mL X-glucuronide) at 37°C overnight. Samples were then cleared in 70% (v/v)

ethanol. Images taken using a digital camera mounted on a dissection microscope (SMZ1500; Nikon) were assembled using Adobe Photoshop.

#### Subcellular Localization of FCL1

To generate the *FCL1-GFP* fusion construct, the coding region of the full-length *FCL1* cDNA without the stop codon was amplified using primers FCL1-F and FCL1-R and cloned into pENTR/D vector using TOPO cloning technology (Invitrogen). Subsequently, the *FCL1* ORF was cloned into pMDC83 vector using LR clonase II (Invitrogen). The final construct was introduced into the *A. tumefaciens* GV3101 strain and then used to infiltrate tobacco leaves. FCL1-GFP signal was examined using a confocal laser scanning microscope (TCS SP2 AOBS; Leica). Primer sequences are listed in Supplemental Table 4 online.

#### Phylogenetic Analysis

Phylogenetic trees were constructed using neighbor-joining, maximum parsimony, and UPGMA algorithms implemented in the MEGA software suite (Tamura et al., 2007) (<http://www.megasoftware.net/>) with 1000 bootstrap replications. Multiple sequences were aligned using ClustalX (Thompson et al., 1994).

#### Yeast Two-Hybrid Assay

The Matchmaker Gold System (Clontech) was used in yeast two-hybrid assays. The coding sequence of *FCL1* was PCR amplified from cDNA templates, cloned into the pGBKT7 vector, and used as the bait. Coding sequences of *STM*, *BP*, *KNAT2*, *KNAT3*, *KNAT4*, *KNAT5*, *KNAT6*, *KNAT7*, *KNATM-B*, *SAW1*, *SAW2*, *BEL1*, *PNF*, *PNY*, *KNOX1*, *KNOX2*, *KNOX3*, *KNOX4*, *KNOX5*, *KNOX6*, *FCL1*, *SGL1*, and *PALM1* were PCR amplified from cDNA templates, cloned into the pGADT7 vector, and used as prey. Positive clones grown on double selection media (SD-Leu-Trp) were tested on three different media (quadra dropout [QD], QD + aureobasidin A [AbA], QD + AbA + X-α-gal) for protein-protein interactions and subsequent quantification of the X-α-galactosidase activity following the manufacturer's instructions (Clontech). All primers used for PCR amplification are listed in Supplemental Table 4 online.

#### Accession Numbers

Sequence data from this article can be found in the Arabidopsis Genome Initiative or NCBI GenBank under the following accession numbers: FCL1 (HQ695002), Gm FCL1 (HQ695005), Gm FCL2 (HQ695006), Lj FCL1 (HQ695007), Os FCL1 (HQ695003), Os FCL2 (HQ695004), Zm FCL1 (HQ695008), Pt FCL1 (JN794532), Vv FCL1 (JN794533), Mt KNOX1 (EF128056.1), Mt KNOX2 (EF128057.1), Mt KNOX3 (EF128058.1), Mt KNOX4 (EF128059.1), Mt KNOX5 (EF128060.1), Mt KNOX6 (EF128061.1), SGL1/UNI (AY928184.1), PALM1 (HM038482.1), PTS/TKD1 (EU352653.1), KNATM-B (NM\_001160868.1), PNY (AT5G02030), PNF (AT2G27990), SAW1 (AT4G36870), SAW2 (AT2G23760), BEL1 (AT5G41410), STM (AT1G62360), BP/KNAT1 (AT4G08150), KNAT2 (AT1G70510), KNAT6 (AT1G23380), KNAT3 (AT5G25220), KNAT4 (AT5G11060), KNAT5 (AT4G32040), and KNAT7 (AT1G62990).

#### Supplemental Data

The following materials are available in the online version of this article.

**Supplemental Figure 1.** The Genetic Map Position of the *fc1* Locus on Chromosome 6

**Supplemental Figure 2.** Confirmation of Deletion Junctions and Expression Analysis of Genes Deleted in *fc1-1* and *fc1-2* Alleles.

**Supplemental Figure 3.** Allelic Series of *fc1* Mutants.

**Supplemental Figure 4.** Compound Leaf Phenotypes of the *fc1-4* Mutant.

**Supplemental Figure 5.** Genetic Complementation of *fc1-1*.

**Supplemental Figure 6.** Zinc Finger Domain Transcription Factor Medtr6g080720 Did Not Rescue *fc1-1* Compound Leaf Defects.

**Supplemental Figure 7.** Full-Length *FCL1* cDNA and the Deduced Amino Acid Sequences.

**Supplement Figure 8.** Amino Acid Sequence Alignments of FCL1 and Its Close Homologs.

**Supplemental Figure 9.** Microarray-Based in Silico Analysis of *FCL1* Tissue-Specific Expression.

**Supplemental Figure 10.** Quantitative RT-PCR Analysis of *KNOX2* and *KNOX6* Expression in the Wild Type and the *fc1-1* Mutant.

**Supplemental Table 1.** Segregation Ratio of *fc1-2* Mutants in F2 Mapping Populations.

**Supplemental Table 2.** Recombination Frequency and Genetic Distance between the *fc1-2* Locus and Molecular Markers on Chromosome 6.

**Supplemental Table 3.** Genotypes of 20 *fc1-2* Mutant Plants That Carry Recombination between *fc1* and Closely Linked Markers.

**Supplemental Table 4.** Primer Sequences Used in This Study.

**Supplemental Table 5.** *Arabidopsis thaliana* Homologs of Deleted Genes in *fc1* Mutants.

**Supplemental Table 6.** Double Mutant Analyses of F2 Plants.

**Supplemental Data Set 1.** Amino Acid Sequence Alignment of FCL1 with PTS, KNATM-B, and the MEINOX Domain of Six Canonical KNOX Proteins from *Medicago truncatula*.

## ACKNOWLEDGMENTS

We thank members of the Chen laboratory for helpful discussions and comments on the manuscript. We also thank Junying Ma and Yuhong Tang, Jianghua Chen, Xiaofei Cheng and Jiangqi Wen, and Shuirong Zhang for assistance with RNA in situ hybridization, scanning electron microscopy, reverse genetic screens, and plant care, respectively, as well as Douglas Cook and Kirankumar Mysore for providing BAC clones and *Tnt1* lines, respectively. Financial support for work done in the Chen laboratory was provided in part by the Samuel Roberts Noble Foundation and the National Science Foundation (DBI 0703285).

## AUTHOR CONTRIBUTIONS

J.P., J.Y., H.W., and R.C. designed the research. J.P., J.Y., H.W., Y.G., and G.L. performed the experiments. J.P., J.Y., H.W., G.B., and R.C. analyzed the data. J.P. and R.C. wrote the article.

Received July 11, 2011; revised October 7, 2011; accepted October 31, 2011; published November 11, 2011.

## REFERENCES

- Allard, R.W. (1956). Formulas and tables to facilitate the calculation of recombination values in heredity. *Hilgardia* **24**: 235–278.
- Altschul, S.F., Madden, T.L., Schäffer, A.A., Zhang, J., Zhang, Z., Miller, W., and Lipman, D.J. (1997). Gapped BLAST and PSI-BLAST: A new generation of protein database search programs. *Nucleic Acids Res.* **25**: 3389–3402.
- Asano, T., Masuda, D., Yasuda, M., Nakashita, H., Kudo, T., Kimura, M., Yamaguchi, K., and Nishiuchi, T. (2008). AtNFXL1, an Arabidopsis homologue of the human transcription factor NF-X1, functions as a negative regulator of the trichothecene phytotoxin-induced defense response. *Plant J.* **53**: 450–464.
- Barkoulas, M., Hay, A., Kougioumoutzi, E., and Tsiantis, M. (2008). A developmental framework for dissected leaf formation in the *Arabidopsis* relative *Cardamine hirsuta*. *Nat. Genet.* **40**: 1136–1141.
- Benedito, V.A., et al. (2008). A gene expression atlas of the model legume *Medicago truncatula*. *Plant J.* **55**: 504–513.
- Berger, Y., Harpaz-Saad, S., Brand, A., Melnik, H., Sirding, N., Alvarez, J.P., Zinder, M., Samach, A., Eshed, Y., and Ori, N. (2009). The NAC-domain transcription factor GOBLET specifies leaflet boundaries in compound tomato leaves. *Development* **136**: 823–832.
- Bharathan, G., Goliber, T.E., Moore, C., Kessler, S., Pham, T., and Sinha, N.R. (2002). Homologies in leaf form inferred from *KNOX1* gene expression during development. *Science* **296**: 1858–1860.
- Blein, T., Pulido, A., Vialette-Guiraud, A., Nikovics, K., Morin, H., Hay, A., Johansen, I.E., Tsiantis, M., and Laufs, P. (2008). A conserved molecular framework for compound leaf development. *Science* **322**: 1835–1839.
- Champagne, C., and Sinha, N. (2004). Compound leaves: Equal to the sum of their parts? *Development* **131**: 4401–4412.
- Champagne, C.E., Goliber, T.E., Wojciechowski, M.F., Mei, R.W., Townsley, B.T., Wang, K., Paz, M.M., Geeta, R., and Sinha, N.R. (2007). Compound leaf development and evolution in the legumes. *Plant Cell* **19**: 3369–3378.
- Chen, J., et al. (2010). Control of dissected leaf morphology by a Cys(2) His(2) zinc finger transcription factor in the model legume *Medicago truncatula*. *Proc. Natl. Acad. Sci. USA* **107**: 10754–10759.
- Chen, J.J., Janssen, B.J., Williams, A., and Sinha, N. (1997). A gene fusion at a homeobox locus: Alterations in leaf shape and implications for morphological evolution. *Plant Cell* **9**: 1289–1304.
- Cheng, X., Wen, J., Tadege, M., Ratet, P., and Mysore, K.S. (2011). Reverse genetics in *Medicago truncatula* using *Tnt1* insertion mutants. *Methods Mol. Biol.* **678**: 179–190.
- Coen, E.S., Romero, J.M., Doyle, S., Elliott, R., Murphy, G., and Carpenter, R. (1990). *floricaula*: A homeotic gene required for flower development in *Antirrhinum majus*. *Cell* **63**: 1311–1322.
- Cosson, V., Durand, P., d'Erfurth, I., Kondorosi, A., and Ratet, P. (2006). *Medicago truncatula* transformation using leaf explants. *Methods Mol. Biol.* **343**: 115–127.
- DeMason, D.A., and Chawla, R. (2004). Roles for auxin during morphogenesis of the compound leaves of pea (*Pisum sativum*). *Planta* **218**: 435–448.
- Di Giacomo, E., Sestili, F., Iannelli, M.A., Testone, G., Mariotti, D., and Frugis, G. (2008). Characterization of *KNOX* genes in *Medicago truncatula*. *Plant Mol. Biol.* **67**: 135–150.
- Dong, Z.C., Zhao, Z., Liu, C.W., Luo, J.H., Yang, J., Huang, W.H., Hu, X.H., Wang, T.L., and Luo, D. (2005). Floral patterning in *Lotus japonicus*. *Plant Physiol.* **137**: 1272–1282.
- Efroni, I., Eshed, Y., and Lifschitz, E. (2010). Morphogenesis of simple and compound leaves: A critical review. *Plant Cell* **22**: 1019–1032.
- Efroni, I., Blum, E., Goldshmidt, A., and Eshed, Y. (2008). A protracted and dynamic maturation schedule underlies *Arabidopsis* leaf development. *Plant Cell* **20**: 2293–2306.
- Ge, L., Chen, J., and Chen, R. (2010). *Palmate-like Pentafoliata1* encodes a novel Cys(2)His(2) zinc finger transcription factor essential for compound leaf morphogenesis in *Medicago truncatula*. *Plant Signal. Behav.* **5**: 1134–1137.
- Hagemann, W., and Gleissberg, S. (1996). Organogenetic capacity of

- leaves: The significance of marginal blastozones in angiosperms. *Plant Syst. Evol.* **199**: 121–152.
- Hareven, D., Gutfinger, T., Parnis, A., Eshed, Y., and Lifschitz, E.** (1996). The making of a compound leaf: Genetic manipulation of leaf architecture in tomato. *Cell* **84**: 735–744.
- Hay, A., and Tsiantis, M.** (2006). The genetic basis for differences in leaf form between *Arabidopsis thaliana* and its wild relative *Cardamine hirsuta*. *Nat. Genet.* **38**: 942–947.
- Hinze, K., Thompson, R.D., Ritter, E., Salamini, F., and Schulze-Lefert, P.** (1991). Restriction fragment length polymorphism-mediated targeting of the *ml-o* resistance locus in barley (*Hordeum vulgare*). *Proc. Natl. Acad. Sci. USA* **88**: 3691–3695.
- Hofer, J., Gourlay, C., Michael, A., and Ellis, T.H.** (2001). Expression of a class 1 knotted1-like homeobox gene is down-regulated in pea compound leaf primordia. *Plant Mol. Biol.* **45**: 387–398.
- Hofer, J., Turner, L., Hellens, R., Ambrose, M., Matthews, P., Michael, A., and Ellis, N.** (1997). *UNIFOLIATA* regulates leaf and flower morphogenesis in pea. *Curr. Biol.* **7**: 581–587.
- Janssen, B.J., Lund, L., and Sinha, N.** (1998). Overexpression of a homeobox gene, *LeT6*, reveals indeterminate features in the tomato compound leaf. *Plant Physiol.* **117**: 771–786.
- Jefferson, R.A., Kavanagh, T.A., and Bevan, M.W.** (1987). GUS fusions: Beta-glucuronidase as a sensitive and versatile gene fusion marker in higher plants. *EMBO J.* **6**: 3901–3907.
- Kaplan, D.R.** (2001). Fundamental concepts of leaf morphology and morphogenesis: A contribution to the interpretation of molecular genetic mutants. *Int. J. Plant Sci.* **162**: 465–474.
- Kimura, S., Koenig, D., Kang, J., Yoong, F.Y., and Sinha, N.** (2008). Natural variation in leaf morphology results from mutation of a novel *KNOX* gene. *Curr. Biol.* **18**: 672–677.
- Koenig, D., Bayer, E., Kang, J., Kuhlemeier, C., and Sinha, N.** (2009). Auxin patterns *Solanum lycopersicum* leaf morphogenesis. *Development* **136**: 2997–3006.
- Koornneef, M., van Eden, J., Hanhart, C.J., Stam, P., Braaksma, F.J., and Feenstra, W.J.** (1983). Linkage map of *Arabidopsis thaliana*. *Heredity* **74**: 265–272.
- Kumar, R., Kushalappa, K., Godt, D., Pidkowich, M.S., Pastorelli, S., Hepworth, S.R., and Haughn, G.W.** (2007). The *Arabidopsis* BEL1-LIKE HOMEODOMAIN proteins SAW1 and SAW2 act redundantly to regulate *KNOX* expression spatially in leaf margins. *Plant Cell* **19**: 2719–2735.
- Laxmi, A., Pan, J., Morsy, M., and Chen, R.** (2008). Light plays an essential role in intracellular distribution of auxin efflux carrier PIN2 in *Arabidopsis thaliana*. *PLoS One* **3**: e1510.
- Lincoln, C., Long, J., Yamaguchi, J., Serikawa, K., and Hake, S.** (1994). A *knotted1*-like homeobox gene in *Arabidopsis* is expressed in the vegetative meristem and dramatically alters leaf morphology when overexpressed in transgenic plants. *Plant Cell* **6**: 1859–1876.
- Lisso, J., Altmann, T., and Müssig, C.** (2006). The *AtNFXL1* gene encodes a NF-X1 type zinc finger protein required for growth under salt stress. *FEBS Lett.* **580**: 4851–4856.
- Long, J.A., Moan, E.I., Medford, J.I., and Barton, M.K.** (1996). A member of the KNOTTED class of homeodomain proteins encoded by the *STM* gene of *Arabidopsis*. *Nature* **379**: 66–69.
- Magnani, E., and Hake, S.** (2008). *KNOX* lost the *OX*: The *Arabidopsis* *KNATM* gene defines a novel class of *KNOX* transcriptional regulators missing the homeodomain. *Plant Cell* **20**: 875–887.
- Molinero-Rosales, N., Jamilena, M., Zurita, S., Gómez, P., Capel, J., and Lozano, R.** (1999). *FALSIFLORA*, the tomato orthologue of *FLORICAULA* and *LEAFY*, controls flowering time and floral meristem identity. *Plant J.* **20**: 685–693.
- Parnis, A., Cohen, O., Gutfinger, T., Hareven, D., Zamir, D., and Lifschitz, E.** (1997). The dominant developmental mutants of tomato, *Mouse-ear* and *Curl*, are associated with distinct modes of abnormal transcriptional regulation of a *Knotted* gene. *Plant Cell* **9**: 2143–2158.
- Peng, J., and Chen, R.** (2011). Auxin efflux transporter MtPIN10 regulates compound leaf and flower development in *Medicago truncatula*. *Plant Signal. Behav.* **6**: 1537–1544.
- Poethig, R.S.** (1997). Leaf morphogenesis in flowering plants. *Plant Cell* **9**: 1077–1087.
- Ramakers, C., Ruijter, J.M., Deprez, R.H., and Moorman, A.F.** (2003). Assumption-free analysis of quantitative real-time polymerase chain reaction (PCR) data. *Neurosci. Lett.* **339**: 62–66.
- Rozen, S., and Skaletsky, H.** (2000). Primer3 on the WWW for general users and for biologist programmers. *Methods Mol. Biol.* **132**: 365–386.
- Saghai-Marooif, M.A., Soliman, K.M., Jorgensen, R.A., and Allard, R.W.** (1984). Ribosomal DNA spacer-length polymorphisms in barley: Mendelian inheritance, chromosomal location, and population dynamics. *Proc. Natl. Acad. Sci. USA* **81**: 8014–8018.
- Shani, E., Ben-Gera, H., Shleizer-Burko, S., Burko, Y., Weiss, D., and Ori, N.** (2010). Cytokinin regulates compound leaf development in tomato. *Plant Cell* **22**: 3206–3217.
- Shani, E., Burko, Y., Ben-Yaakov, L., Berger, Y., Amsellem, Z., Goldshmidt, A., Sharon, E., and Ori, N.** (2009). Stage-specific regulation of *Solanum lycopersicum* leaf maturation by class 1 KNOTTED1-LIKE HOMEODOMAIN proteins. *Plant Cell* **21**: 3078–3092.
- Tadege, M., Wen, J., He, J., Tu, H., Kwak, Y., Eschstruth, A., Cayrel, A., Endre, G., Zhao, P.X., Chabaud, M., Ratet, P., and Mysore, K.S.** (2008). Large-scale insertional mutagenesis using the *Tnt1* retrotransposon in the model legume *Medicago truncatula*. *Plant J.* **54**: 335–347.
- Tamura, K., Dudley, J., Nei, M., and Kumar, S.** (2007). MEGA4: Molecular Evolutionary Genetics Analysis (MEGA) software version 4.0. *Mol. Biol. Evol.* **24**: 1596–1599.
- Thompson, J.D., Higgins, D.G., and Gibson, T.J.** (1994). CLUSTAL W: Improving the sensitivity of progressive multiple sequence alignment through sequence weighting, position-specific gap penalties and weight matrix choice. *Nucleic Acids Res.* **22**: 4673–4680.
- van Ooijen, J., and Voorrips, R.** (2001). JoinMap3.0 Software for Calculation of Genetic Linkage Maps. (Wageningen, The Netherlands: Plant Research International).
- Wang, H., Chen, J., Wen, J., Tadege, M., Li, G., Liu, Y., Mysore, K.S., Ratet, P., and Chen, R.** (2008). Control of compound leaf development by *FLORICAULA/LEAFY* ortholog *SINGLE LEAFLET1* in *Medicago truncatula*. *Plant Physiol.* **146**: 1759–1772.
- Wang, H., Jones, B., Li, Z., Frasse, P., Delalande, C., Regad, F., Chaabouni, S., Latché, A., Pech, J.C., and Bouzayen, M.** (2005). The tomato Aux/IAA transcription factor IAA9 is involved in fruit development and leaf morphogenesis. *Plant Cell* **17**: 2676–2692.
- Wang, H., Li, G., and Chen, R.** (2006). Fast neutron bombardment (FNB) induced deletion mutagenesis for forward and reverse genetic studies in plants. In *Floriculture, Ornamental and Plant Biotechnology: Advances and Topical Issues*, 1st ed. J. Teixeira da Silva, ed (Isleworth, UK: Global Science Books), pp. 629–639.
- Yu, J.B., Bai, G.H., Cai, S.B., and Ban, T.** (2006). Marker-assisted characterization of Asian wheat lines for resistance to *Fusarium* head blight. *Theor. Appl. Genet.* **113**: 308–320.
- Zhou, C., Han, L., Hou, C., Metelli, A., Qi, L., Tadege, M., Mysore, K.S., and Wang, Z.Y.** (2011). Developmental analysis of a *Medicago truncatula* *smooth leaf margin1* mutant reveals context-dependent effects on compound leaf development. *Plant Cell* **23**: 2106–2124.